PHYSICAL REVIEW B, VOLUME 64, 140101(R)

# Characterization of the metallic phases in $BaCo_{0.9}Ni_{0.1}S_{1.87}$

J.-S. Zhou, W. J. Zhu, and J. B. Goodenough
*Texas Materials Institute, ETC 9.102, University of Texas, Austin, Texas 78712*
(Received 1 March 2001; revised manuscript received 27 June 2001; published 17 September 2001)

The temperature dependence of the resistivity along the *c* axis and in the *a-b* plane of layered $BaCo_{0.9}Ni_{0.1}S_{1.87}$ has been measured on a single crystal under hydrostatic pressures. The monoclinic metallic (LTM) phase stable at $T \leqslant 150$ K is suppressed under a pressure $P > 1.5$ kbar; it has a nearly isotropic conductivity. Pressure induces an insulator-metal (IM) transition at $P > 10$ kbar within the tetragonal phase. A change from a nearly isotropic conduction to a highly anisotropic conduction is associated with the IM transition. Isotropic conduction in the LTM phase is consistent with its crystallographic structure; the IM transition in the tetragonal phase has been interpreted to be due to a high-spin to low-spin transition of Co(II) ions. The resistivity and thermal conductivity of the LTM metallic phase are typical of those of a normal metal.

DOI: 10.1103/PhysRevB.64.140101 PACS number(s): 71.30.+h, 72.80.Ga, 73.21.−b, 71.28.+d

In a search for new high-temperature superconductors among layered compounds other than the copper oxides, Martinson and Schweitzer[1] found a first-order metal-insulator transition at $T_t \approx 180$ K on cooling in the compound $BaCo_{1-x}Ni_xS_{2-y}$ ($x=0.1$). The physical origin of the metallic phase has, however, remained a mystery. Hydrostatic pressure, which normally stabilizes the metallic phase at an isostructural transition, suppresses the low-temperature metallic phase in $BaCo_{1-x}Ni_xS_{2-y}$.[2] Moreover, infrared data[3] have revealed not only a strong coupling of the symmetric in-plane phonon modes to an electronic excitation, but also an extremely small ratio of carrier density to effective mass in the metallic phase.

Tetragonal $BaCo_{1-x}Ni_xS_2$ contains $Co_{1-x}Ni_xS$ sheets alternating with rock-salt BaS planes.[4] The $Co_{1-x}Ni_x$ atoms occupy square-pyramidal sites, having their apical anions alternating above and below a square array of sulfur atoms in the S basal planes. Whereas $BaNiS_2$ is a Pauli paramagnetic metal, $BaCoS_2$ is a Mott insulator with an antiferromagnetic Néel temperature $T_N = 310$ K. A continuous change in lattice parameters with *x* indicates a complete solid solution, but an insulator-metal transition occurs at a critical value $x_c \approx 0.22$.[5] With $x < x_c$, the introduction of sulfur vacancies introduces the first-order transition to a metallic phase below $T_t \approx 180$ K that was observed by Martinson and Schweitzer. After our investigation had begun, a study[6] of Se substitution for S in $BaCo_{0.9}Ni_{0.1}S_{2-y}Se_y$ clarified two critical issues: (a) the negative chemical pressure introduced by Se substitution stabilizes the metallic phase appearing below $T_t$ (anion vacancies are not necessary), and (b) the high-temperature-tetragonal (HTT) phase at $T > T_t$ is to be distinguished from the low-temperature-monoclinic (LTM) phase at $T < T_t$. In the monoclinic phase, a cooperative crystallographic shear within the $Co_{1-x}Ni_xS$ sheets transforms the edge-shared square-pyramidal sites to pairs of edge-shared tetrahedral sites with an associated increase in volume per formula unit.

A band calculation for metallic $BaNiS_2$ (Ref. 7) places the Fermi energy $\varepsilon_F$ in a partially filled, antibonding $(x^2-y^2)$ $\sigma^*$ band that overlaps $(z^2-r^2)$ and $(yz \pm izx)$ subbands. We should, therefore, anticipate a strongly anisotropic conductivity in the metallic tetragonal phase with $\rho_c \gg \rho_{ab}$. A band calculation for the LTM phase is not yet available. In order to distinguish between the tetragonal and monoclinic metallic phases, we have undertaken a study of the transport properties of single-crystal $BaCo_{0.9}Ni_{0.1}S_{1.87}$ samples under pressure. We demonstrate a crossover from an isotropic three-dimensional (3D) conductivity in the insulating HTT phase to a strongly anisotropic 2D conductivity in the metallic HTT phase. We have also measured the thermal conductivity of the LTM phase of $BaCo_{0.9}Ni_{0.1}S_{1.87}$ to provide additional information for interpreting the metallic conduction.

Single crystals of $BaCo_{0.9}Ni_{0.1}S_{1.87}$ were grown by vapor transport from a starting charge of $BaCo_{0.92}Ni_{0.08}S_2$. A *ca.* 2-g pellet of the charge material was placed at one end of a 5-cm-long quartz tube that was then sealed under a vacuum of $10^{-3}$ Torr. The sealed tube was loaded into a tube furnace with the pellet located at the center of the hot zone. The sealed tube was heated at a rate of 250 °C/h to 1050 °C, held at this temperature for 2 h before cooling at 2 °C/h to 950 °C, and finally quenched in water. Black, platelike crystals as large as 5 mm×5 mm×0.1 mm formed at the cooler end of the tube. A 1.0 mm×0.5 mm×0.05 mm crystal portion having a mirrorlike surface was chosen for measurements of transport properties under pressure and thermal conductivity. The Ni concentration $x \approx 0.1$ in the crystal was determined from the Néel temperature $T_N$ in accordance with the plot of $T_N$ versus *x* established[1] for $BaCo_{1-x}Ni_xS_2$. The as-grown crystals were insulators and showed no transition to the LTM phase down to lowest temperatures. In order to introduce sulfur vacancies, the crystals were sealed in a quartz tube under $10^{-3}$ Torr together with a polycrystalline sample of $BaCo_{0.9}Ni_{0.1}S_{1.87}$ and heated to 920 °C followed by an anneal at 500 °C for 6 h. The resulting sulfur deficiency of a crystal was taken to be the same, $y = 0.13$, as that of the polycrystalline material with which it was equilibrated. The sulfur deficiency of the polycrystalline material was determined by a standard atomic-emission spectrum.

A four-probe method was used to measure the resistivity under pressure. Cu wires (0.0005 in. diam.) were attached to the crystals with silver epoxy. The measurements under pressure were carried out on a self-clamped Be-Cu cell using silicone oil as a pressure medium. The brittle crystals shattered into small pieces after one or two thermal cycles

 

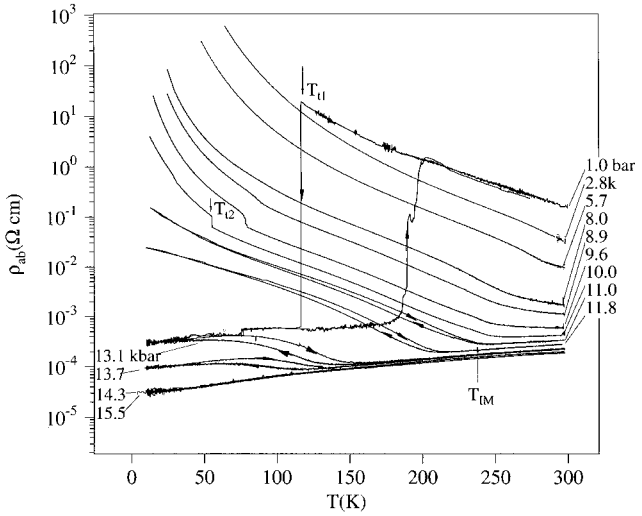


FIG. 1. The temperature dependence of resistivity along the *a-b* plane under pressure in single-crystal $BaCo_{0.9}Ni_{0.1}S_{1.87}$. $T_{t1}$: critical temperature of the structural transition from the HTT to the LTM phase; $T_{t2}$: temperature of the insulator-to-insulator transition; $T_{IM}$: temperature of the metal-insulator transition in the HTT phase. Pressures labeled have been measured at room temperature.

through $T_t$. However, the crystals retain their shape over many thermal cycles if kept under a pressure of several tens of atmospheres. The original $\rho(T)$ is reproducible after the pressure is released from a high value to a lower one greater than ambient. The thermal conductivity was measured by means of a steady-state method.

The resistivity data of Fig. 1 and Fig. 2 exhibit several features that, to the best of our knowledge, have not been observed in previous reports on ceramic samples: (a) the metal-insulator transition at $T_{t1}$ is so sharp that essentially no data points were recorded in a small temperature interval $\Delta T = 0.05$ K that spanned $T_{t1}$; (b) the resistivity changes by four orders of magnitude on crossing $T_{t1}$; (c) an insulator-insulator transition, more visible in $\rho_{ab}(T)$, occurs at $T_{t2}$ at pressures $P > 8.0$ kbar measured at room temperature (the transition shows a pressure hysteresis); (d) pressure induces a

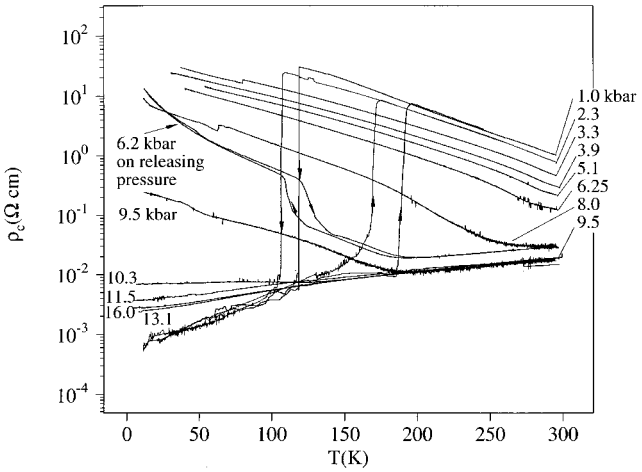


FIG. 2. The same as Fig. 1 along the *c* axis.

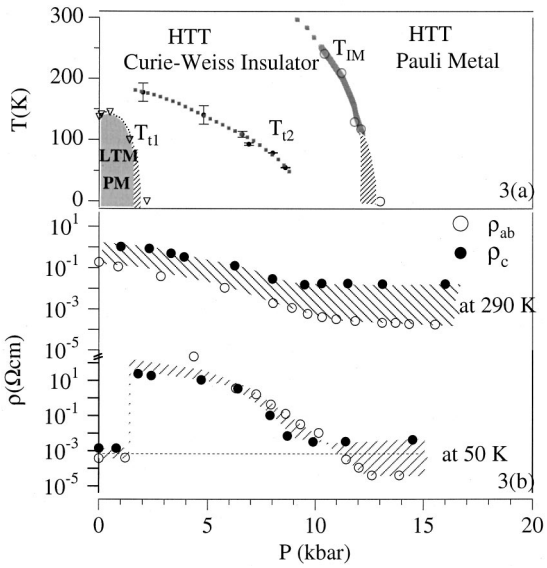


FIG. 3. (a) The pressure dependence of the critical temperatures $T_{t1}$, $T_{t2}$, $T_{IM}$, and (b) the resistivity at 290 and 50 K. $T_{t2}$ is taken from the curves of $\rho_{ab}$ versus $T$ under different pressures. Pressures have been measured at the critical temperatures in Fig. 3(a), and at 290 and 50 K in Fig. 3(b). PM stands for Pauli paramagnetic metal. LTM phase is shaded with dark gray.

first-order insulator-metal transition in the HTT phase at a $T_{IM}$ that decreases with increasing pressure; (e) the resistivity of the HTT phase below $T_{IM}$ decreases with increasing pressure until it becomes metallic before $T_{IM}$ falls to zero; (f) $\rho_c$ of the metallic LTM phase is lower than $\rho_c$ of the metallic HTT phase, but the opposite is found for $\rho_{ab}(T)$. The pressure dependence of the critical temperatures is summarized in the *P-T* phase diagram of Fig. 3(a), and the $\rho_{ab}$-*P*, $\rho_c$-*P* plots obtained at 50 and 290 K are shown in Fig. 3(b) in order to demonstrate the crossover from 3D to 2D conductivity in the HTT phase. An accurate calculation of the ratio between $\rho_c$ and $\rho_{ab}$ becomes impossible because of errors in the measurement of resistivity. However, the change of this ratio under pressure is highly reliable. From the curves of $\rho_c$ and $\rho_{ab}$ at 290 K, which are within the HTT phase according to Fig. 3(a), a ratio of $\rho_c/\rho_{ab} \approx 10$ remains throughout the insulating phase and changes to 100 in the metallic phase. The ratio at 50 K looks complicated as pressure introduces three phase transitions, as is shown in Fig. 3(a). A change in the ratio of $\rho_c/\rho_{ab}$ from 3 in the LTM phase to 100 in the metallic HTT phase has been found. The ratio becomes unreliable in the insulating HTT phase because an insulator to insulator transition at $T_{12}$ appears to be highly sensitive to shear strain in the pressure medium, which makes it difficult to duplicate the strain state in the measurements of $\rho_c$ and $\rho_{ab}$. It is interesting to compare the metallic LTM phase and the metallic HTT phase. Both phases fall into the "bad metal" regime. In both phases, $\rho_c$ is higher than $\rho_{ab}$. However, the LTM phase is more conductive along the *c* axis than the HTT phase.

In order to understand these transport properties, we begin with the crystallographic structures of the *MS* sheets shown in Fig. 4. Schematic one-electron representations of the an-

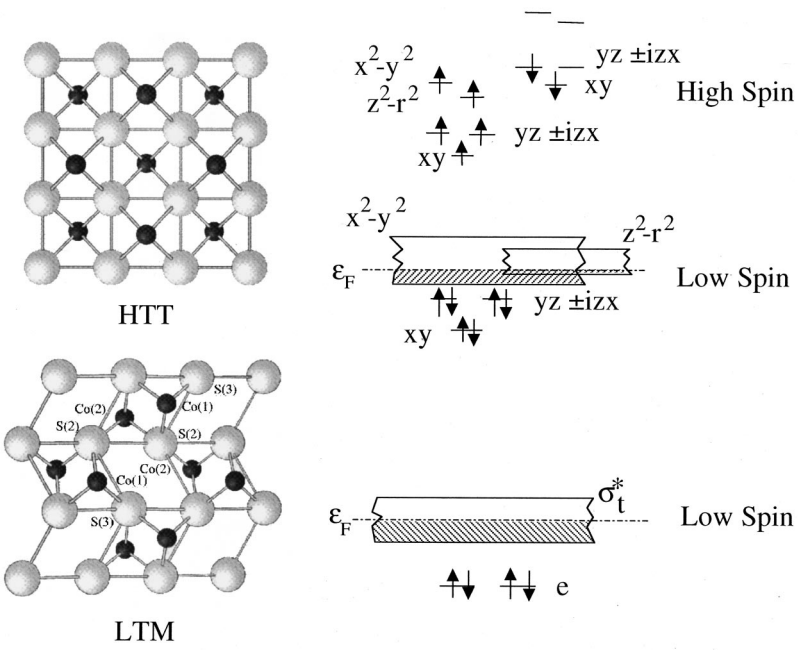


FIG. 4. The crystallographic structures (after Ref. 6) of the high-temperature tetragonal phase and the low-temperature monoclinic phase; schematic energy diagrams are also shown.

tibonding states of Co(II)-3*d* parentage are also shown. Neutron-diffraction data[8] have shown that the Co(II) of $BaCoS_2$ have a localized high-spin configuration with $S=\frac{3}{2}$. In our compound, the ambient-pressure HTT phase would also have a localized high-spin configuration on the Co(II). In the metallic HTT phase, stronger Co-S covalent bonding raises the majority-spin $(x^2-y^2)$ level above the minority-spin $(yz\pm izx)$ level, which fills all the *xy*, $(yz\pm izx)$ orbitals with spin-paired electrons. The transition to low-spin Co(II) also transforms the localized $(x^2-y^2)$ level into a narrow $\sigma^*$ band of itinerant-electron states that overlaps the $(z^2-r^2)$ level. With the transfer of $(z^2-r^2)$ electrons to the $\sigma^*$ band, the spin degeneracy of the $(z^2-r^2)$ level is no longer lifted. The Ni atoms and sulfur vacancies are electron donors that perturb the periodic potential, but the Fermi energy $\varepsilon_F$ lies above any mobility edge in the $\sigma^*$ band. The tetragonal structure allows Co-S-Co interactions in the basal planes, but only Co-S-S-Co interactions for *c* axis conduction. Therefore, a highly anisotropic resistivity with $\rho_{ab}\ll\rho_c$ follows directly from the model of a high-spin to low-spin transition that contracts the volume of the HTT phase but does not change the symmetry. Therefore, high pressure stabilizes the metallic low-spin HTT phase. In the LTM phase, on the other hand, the tetrahedral-site Co(II) have spin-paired *e* electrons and a little more than half-filled $\sigma_t^*$ band of *t*-orbital parentage that is connected in 3D. In this case, filled *e* orbitals prevent metal-metal bonding across the shared tetrahedral-site edge and a nearly isotropic conductivity is due to electrons in the $\sigma_t^*$ band. As in the LTM phase, the high-spin state of the HTT insulator phase provides electron transport via partially occupied *t* orbitals, which allows more isotropic conduction via the sulfur atoms than does conduction in an $(x^2-y^2)$ band.

The pressure-induced insulator-metal transition in the HTT phase is not like that predicted by Mott and Hubbard; it is a transition from a high-spin Mott-Hubbard insulator to a low-spin metallic phase that appears to go in two steps. The decrease in resistivity with pressure on the approach to the metallic phase in the interval $T_{t2}<T<T_{\rm IM}$ of the intermediate step is similar to that found in the insulator phase of $PrNiO_3$, where the insulator phase also becomes metallic under pressure while the transition temperature remains finite. The insulator phase in $PrNiO_3$ was interpreted to be a long-range ordering of strong-correlation fluctuations already present in an itinerant-electron matrix in the metallic phase.[9]

Finally, we turn to the character of the 3D metallic conduction in the more-than-half-filled $\sigma_t^*$ band of the LTM phase. We found the basal-plane thermoelectric power to be small and negative, which indicates a deep minimum in the density of states in the middle of the $\sigma_t^*$ band as a result of intra-atomic electron-electron interactions. The $\sigma_t^*$ bands are antibonding with respect to the Co-S interactions, but electron correlations within a narrow band may stabilize Co-Co bonding states relative to the Co-Co antibonding states within the band. Although the conductivity is of the same order of magnitude as that of $\rho_{ab}$ in the high-$T_c$ cuprates, the infrared reflectivity gave an anomalously small $\mathrm{nm}_e/\mathrm{m}^*$ ratio for the charge carriers. A small $\mathrm{nm}_e/\mathrm{m}^*$ and a metallic $\sigma=ne^2\tau/\mathrm{m}^*$ would suggest a large mean free path for a few itinerant electrons above a mobility edge, the Ni-atom and sulfur-vacancy donors introducing Anderson-localized states in the middle of the $\sigma_t^*$ band just below the Fermi energy $\varepsilon_F$. It has been suggested[3] that the long mean free path of the electrons is due to a strong coupling to a traveling charge-density wave (CDW). Since electron coupling in a traveling CDW is known[10] to give an enhancement of the thermal conductivity $\kappa(T)$, we decided to determine whether such an enhancement was present in our single crystal.

Figure 5 shows that the $\kappa_{ab}(T)$ of our single crystal is significantly higher than the $\kappa(T)$ obtained[11] on a ceramic sample. The temperature dependence of $\kappa_{ab}(T)$ reveals two significant features: (a) on cooling, $\kappa_{ab}$ jumps abruptly at $T_{t1}$

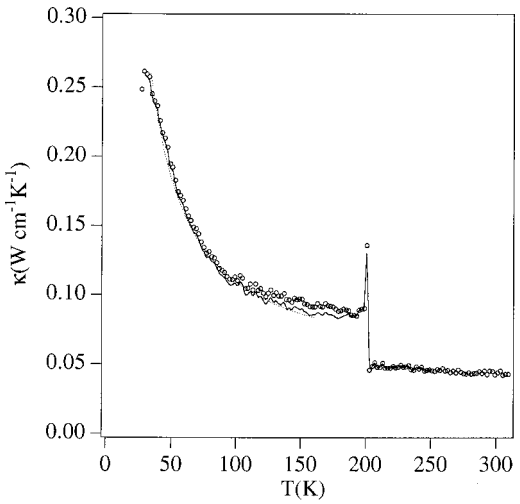


FIG. 5. The temperature dependence of thermal conductivity $\kappa$ in the *a*-*b* plane of a $Ba_{0.9}Ni_{0.1}S_{1.87}$ crystal. Circles represent the $\kappa$ measured; solid line represents the $\kappa$ after correction for the electronic contribution (see text for the detail). The dashed line is a fitting to the power law $\kappa \sim 1/T^{1.1}$.

and (b) $\kappa_{ab}$ increases with decreasing temperature in the LTM phase. In this plot, the upper bound of the electronic contribution obtained from the Wiedemann-Franz (W-F) law is much smaller than the phonon contribution. The jump in $\kappa_{ab}(T)$ on passing from the HTT to the LTM phase at $T_{t1}$ therefore reflects a release of phonons on passing from the localized-electron to the itinerant-electron phase. Both $\kappa_{ab}(T)$ and the lattice contribution to $\kappa_{ab}(T)$, which was obtained by subtracting the electronic contribution as calculated from $\rho_{ab}$ and the W-F law, can be fitted by a power law $\kappa \sim T^{-1.1}$. The relaxation-time-approximation formula is normally used to describe the lattice contribution at low temperatures; at $T \geqslant \theta_D$, the formula can be replaced by a $1/T$ law.[12] Julian[13] has pointed out that in many cases the $1/T$ law remains applicable to temperatures as low as $\theta_D/4$. We have observed a $\kappa \sim 1/T$ in $LaMnO_3$ down to 30 K.[14] The magnitude of $\kappa_{ab}(T)$ is also comparable to that of metallic $BaNiO_3$.[15] Both the temperature dependence and magnitude of $\kappa_{ab}(T)$ in the LTM phase rule out the possibility that a travelling CDW is formed.

In conclusion, $BaCo_{0.9}Ni_{0.1}S_{1.87}$ contains a localized, high-spin $3d$-electron configuration at the Co(II) ions in the antiferromagnetic-insulator HTT phase that is stable above $T_t \approx 150$ K at ambient pressure; it undergoes a first-order transition to a metallic phase in two distinguishable ways. An insulator to metal transition at $T_{t1} \approx 150$ K is accompanied by a structural transition and an insulator to metal transition at $T_{\mathrm{IM}}$ is induced by pressure within the HTT phase. The latter transition is preceded by an insulator-insulator transition that marks the appearance of an intermediate phase in which the resistivity approaches metallic behavior before $T_{\mathrm{IM}}$ is reached. Measurement under pressure of the resistivity of single crystals has not only demonstrated the evolution of the phase transitions as a function of pressure, but also revealed an isotropic conduction in the LTM phase and a crossover from 3D to 2D conduction associated with the IM transition in the HTT phase. At atmospheric pressure, the structure changes on cooling through $T_{t1}$ to the 3D-metallic LTM phase in which the transition-metal atoms are displaced from edge-shared square-pyramidal sites to pairs of edge-shared tetrahedral sites. The volume of the LTM phase is larger than that of the HTT phase, and a modest pressure suppresses the LTM phase. The crossover from 3D to 2D conduction at $T_{\mathrm{IM}}$ allows us to associate the IM transition with a high-spin to low-spin transition within the HTT phases that produces a first-order contraction of the lattice and a delocalization of the electrons in $\sigma$-bonding orbitals. The tetragonal symmetry of the square-pyramidal sites stabilizes the $(z^2-r^2)$ level relative to the $(x^2-y^2)$ level in the HTT insulator phase; in the HTT metallic phase, broadening of the $(x^2-y^2)$ $\sigma^*$ band makes this band overlap the $(z^2-r^2)$ level, which prevents removal of the spin degeneracy of the $(z^2-r^2)$ level. Both the electrical and thermal conductivity of the LTM phase show that its metallic conduction behaves as a normal metal.

We thank the Robert A. Welch Foundation and TCSUH, both of Houston, Texas, and the NSF for financial support.

[1] L. S. Martinson, J. W. Schweitzer, and N. C. Baenziger, Phys. Rev. Lett. **71**, 125 (1993).
[2] C. Looney, J. S. Schilling, L. S. Martinson, and J. W. Schweitzer, Phys. Rev. Lett. **76**, 4789 (1996).
[3] K. H. Kim, Y. H. Kim, L. S. Martinson, and J. W. Schweitzer, Phys. Rev. Lett. **78**, 4498 (1997).
[4] I. E. Grey and H. Steinfink, J. Am. Chem. Soc. **92**, 5093 (1970).
[5] L. S. Martinson, J. W. Schweitzer, and N. C. Baenziger, Phys. Rev. B **54**, 11 265 (1996).
[6] J. W. Schweitzer, L. S. Martinson, N. C. Baenziger, D. C. Swenson, V. G. Young, Jr., and I. Guzei, Phys. Rev. B **62**, 12 792 (2000).
[7] L. F. Mattheiss, Solid State Commun. **93**, 879 (1995).
[8] K. Kodama, S. Shamoto, H. Harashina, J. Takeda, M. Sato, K. Kakurai, and M. Nishi, J. Phys. Soc. Jpn. **65**, 1782 (1996).
[9] J.-S. Zhou, J. B. Goodenough, B. Dabrowski, P. W. Klamut, and Z. Bukowski, Phys. Rev. B **61**, 4401 (2000).
[10] Z. Bhihar, D. Staresinic, K. Kiljakovic, and T. Sambongi, Europhys. Lett. **40**, 73 (1997).
[11] H. Kang, P. Mandal, I. V. Medvedeva, J. Liebe, G. H. Rao, K. Bärner, A. Poddar, and E. Gmelin, J. Appl. Phys. **83**, 6977 (1998).
[12] R. Berman, *Thermal Conductivity in Solids* (Oxford University Press, New York, 1976).
[13] C. L. Julian, Phys. Rev. **137**, A128 (1965).
[14] J.-S. Zhou and J. B. Goodenough, Phys. Rev. B **64**, 024421 (2001).
[15] J. Takeda, J. Sakurai, A. Nakamura, M. Kato, Y. Kobayshi, and M. Sato, J. Phys. Soc. Jpn. **68**, 1602 (1999).